Colloid Polym Sci (2013) 291:1001–1007
DOI 10.1007/s00396-012-2822-8

ORIGINAL CONTRIBUTION

Design and synthesis of the polyaniline interface for polyamide 66/multi-walled carbon nanotube electrically conductive composites

Hua Wang · Lei Wang · Ruoxi Wang · Xingyou Tian · Kang Zheng

Received: 20 July 2012 / Revised: 4 September 2012 / Accepted: 24 September 2012 / Published online: 25 October 2012

Abstract A polyaniline interface had been designed and built between multi-walled carbon nanotubes (MWCNTs) and polyamide 66 (PA66) in order to help in the dispersion of MWCNTs in PA66 and improve the interfacial combination between them. Transmission electron microscopy characterizations indicated that functionalized MWCNTs (f-MWCNTs) could be well-distributed in PA66 matrix and the interfacial boundary between them was indiscernible. The mixing conditions, such as f-MWCNT content, temperature, and mixing speed, played important roles in determining the formation of the conductive network and the electrical conductivities of PA66/f-MWCNT composites synthesized. A continuous conductive network was formed at 10 wt% f-MWCNT content, and the corresponding PA66/f-MWCNT composite exhibited an electrical conductivity of 8 orders of magnitude higher than pure PA66. The conducting mechanism agreed well with a thermal fluctuation-induced tunneling model.

Keywords Carbon nanotubes · Polyamide · Interface · Polyaniline · Miniemulsion polymerization

Introduction

In recent years, carbon nanotubes (CNTs) have been considered as ideal fillers in polymer composites owing to their high aspect ratio, nanosize in diameter, very low density, and, more importantly, excellent mechanical and electrical properties [1, 2]. However, uniform dispersion of CNTs in polymer matrix is restricted presumably due to (a) strong inter-tube van der Waals interaction and (b) lack of interfacial interaction between polymer and CNTs. One of the most widely used approaches for effective dispersion of CNTs in polymer matrix is to introduce functional groups covalently on the surface of CNTs. A common approach to covalent modification of CNTs requires harsh reaction conditions in strong acids such as nitric acid and sulfuric acid or their mixtures at elevated temperatures. A significant damage to the molecular framework of CNTs, such as sidewall opening, breaking, and turning into amorphous carbon, is inevitable. Thus, developing efficient chemical modification methods without or with little damage to the surface of CNTs are very important for the development of the ultimate CNT composites [3, 4].

Polyamide 66 (PA66), an important engineering thermoplastic material with outstanding properties such as high toughness, high tensile strength, high abrasion resistance, low density, and low frictional coefficient, is widely used in many applications, such as tire cord, rope, air bag, conveyer belt, bearing, and gear [5]. However, similar to most polymers, PA66 has a high volume resistivity of $10^{15}\,\Omega$cm, which will bring electrostatic accumulation in its usual applications. The releases of the electrostatic charges may result in damages to machines, pilling of clothes, and even explosion and fire disaster may happen. From this point of review, much attention should be paid to the modification of PA66 by conductive components, and then, the wide range of applications of nylon can be further extended to antistatic packages, electronic component, MEI shielding materials, and so on. As reported, Jo et al. [6] synthesized a new compatibilizer, poly(vinylbenzyloxymethylnaphthalene)-*g*-poly(*t*-butylmethacry-late-co-methacrylicacid), to improve

H. Wang (✉) · L. Wang · X. Tian · K. Zheng
Key Laboratory of Materials Physics,
Institute of Solid State Physics, Chinese Academy of Sciences,
Hefei 230031, China
e-mail: wanghua@issp.ac.cn

R. Wang
Ningbo Institute of Material Technology & Engineering,
Chinese Academy of Sciences,
Ningbo 315040, China

the mechanical and electrical properties of PA66/multi-walled carbon nanotube (MWCNT) composites. Kodgire et al. [7] presented the key role of sodium salt of 6-aminohexanoic acid in assisting in debundling of the MWCNTs through specific interactions leading to homogeneous dispersion within polyamide 6 matrix during melt mixing. Winey [8] adapted interfacial polymerization for PA66, in which single-walled CNTs were incorporated in purified, functionalized, or surfactant-stabilized forms.

The key object of this work is to investigate a simple approach that homogeneous dispersion of MWCNTs in PA66 and strong interface force between them can be realized, at the same time electrical conductive PA66 composite materials could be fabricated. Therefore, we design and synthesize a polyaniline (PANI)-functionalized interface for PA66/MWCNT composites. It has been known that the quinoid ring in the main chain of doped PANI interacts with the surface of MWCNTs by π–π interaction [9, 10] and that the similar polar structure of PANI with PA66 matrix is helpful for excellent interface bonding. It is easily expected that the PANI interface should act as an effective compatibilizer for dispersing MWCNTs in PA66 matrix. An easy method, miniemulsion polymerization, was presented to fabricate functionalized MWCNT (f-MWCNT) composites with good core–shell structures for the first time. The π–π interaction between MWCNTs and PANI was verified by Fourier transform infrared spectroscopy (FT-IR), ultraviolet spectroscopy (UV), and transmission electron microscopy (TEM) characterizations. The effectiveness of the PANI interface for PA66/f-MWCNT composites was examined in terms of the dispersion of MWCNTs in PA66 matrix and the electrical properties of PA66/f-MWCNT composites. Furthermore, the conducting mechanism was primarily studied.

Experimental

Materials

Aniline (An), sodium dodecyl sulfate (SDS), hydrochloric acid (HCl), and ammonium persulfate (APS) were all purchased from Shanghai Chemical Reagents Co., China, and An was distilled and stored in a refrigerator before use. MWCNTs were bought from Chengdu Organic Chemicals Co., Ltd., Chinese Academy of Sciences and used as received. Hexadecane (HD) was a product of Aldrich and was also used directly.

Preparation of f-MWCNT composites

f-MWCNT composites were synthesized by miniemulsion polymerization method. In a typical experiment, 0.5 g MWCNTs, 5 g An, and 0.1 g HD (costabilizer) were mixed in a three-necked flask and stirred for 20 min, followed by sonication for 15 min to obtain well-dispersed suspensions. After that, 20 mL water solution containing 0.1 g SDS was added. The reaction mixture was further stirred and sonicated for 15 min, respectively, to obtain a homogeneous miniemulsion. An then, a 30-mL aqueous solution of 0.1 mol/L HCl dissolving 12.25 g APS, was added dropwisely to the miniemulsion to initiate the polymerization. The polymerization was carried out at room temperature for 6 h in darkness, and the resulting black precipitate was filtered and rinsed with distilled water and methanol for several times, respectively. The remaining filters were f-MWCNT composites, which were further dried under a vacuum at 60 °C for 24 h. And for comparison, a neat PANI specimen was prepared by the same technique without MWCNTs present.

Fabrication of electrical conductive PA66/f-MWCNT composites

Electrical conductive PA66/f-MWCNT composites were prepared by melt compounding in XSS-300 torque rheometer and the products obtained were black cakes. PA66 was dried under vacuum at 80 °C for 8 h before use.

Characterization

Powder X-ray diffraction patterns were recorded with a Japan Rigaku D/max γ_A X-ray diffractometer equipped with graphite monochromatized Cu Kα irradiation (γ=0.154178 nm), employing a scanning rate of 0.02°/s in the 2θ range from 20° to 70°. TEM images were observed on a JEOL-2010 transmission electron microscope with an accelerating voltage of 120 kV. For microtomed samples, the sample powder was embedded into epoxy resin, which was then ultramicrotomed to a thickness of ca. 70 nm. The electrical conductivity at room temperature was measured by a four-point van der Pauw method using a RTS-9 electrometer, and the electrical conductivity at other variable temperature was measured by a Physical Property Measurement System from Quantum Design, USA. The samples were compressed at 280 °C into rectangular shape (approximately 4×2×1.5 mm), obtained by applying a hydraulic pressure of about 10 MPa.

Results and discussion

Fabrication of PANI-functionalized interface by miniemulsion polymerization

Miniemulsions are aqueous dispersions of relatively stable oil droplets with a size in the region of 50–500 nm prepared by shearing a system containing oil, water, surfactant, and a

highly water-insoluble compound called hydrophobe. Recently, miniemulsion polymerization has attracted much attention because of its wide applications in preparation of particles with special morphologies, controlled radical polymerization in dispersed media, encapsulation of inorganic solids with polymers, and so on [11, 12]. It expands the application of emulsion polymerization and provides many advantages. However, to our knowledge, the preparation of PANI f-MWCNTs via miniemulsion polymerization has not been reported in literature. In order to realize homogeneous dispersion of MWCNTs in PA66 and strong interfacial force between them, a PANI interface had been designed and synthesized by miniemulsion polymerization.

It has been known that the quinoid ring in the main chain of doped PANI interacts with the MWCNTs by π–π interactions [13–17]. Both FT-IR and UV spectra have proved this fact (see supporting information). TEM characterizations are applied to study the structures of f-MWCNTs. As indicated in Fig. 1b, c, well-dispersed f-MWCNT composites show uniform core–shell structures with a PANI shell of around 10 nm, while the pristine MWCNTs are clearly evident (Fig. 1a) as endless tangled hollow ropes. The formation mechanism of f-MWCNT composites with the core–shell structures is believed to involve strong π–π interactions between PANI and MWCNTs, which overcome the van der Waals interactions between MWCNTs [18]. Such strong interactions ensure An monomers adsorbing on the surface of MWCNTs, which serve as the core and self-assembly templates during the formation of f-MWCNTs by miniemulsion polymerization.

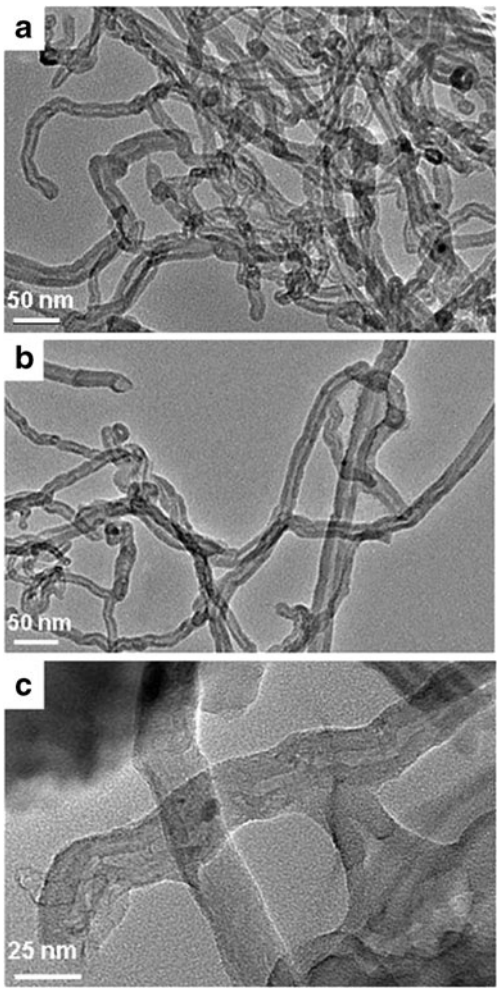

Fig. 1 **a**–**c** TEM characterizations of the structures of f-MWCNTs

To further confirm the validity of the TEM image, the electrical conductivities of PANI and f-MWCNTs are measured according to the standard four-point probe technique. As Table 1 shows, when MWCNT content is 3 %, the electrical conductivity of the composite is 0.03 S/cm, which is five times higher than that of the pure PANI measured under similar conditions. If the MWCNT amount reaches 55 %, the electrical conductivity of f-MWCNTs rises even beyond the pressed pellet of pure MWCNTs (7.41 S/cm). This improvement of electrical conductivity should be attributed to the charge transfer from PANI to MWCNTs, which provides further evidence for the strong π–π interaction between PANI and MWCNTs. In addition, due to the large aspect ratio and surface area of MWCNTs, they may serve as conductive bridges connecting PANI-conducting domains and increase the electrical conductivities of the composites.

Preparation of electrically conductive PA66/f-MWCNT composites

To fabricate electrically conductive PA66/f-MWCNT composites, the major challenge is to achieve a uniform dispersion of MWCNTs in the PA66 polymer matrix. The PANI interface had been built as described above, and the obtained f-MWCNT composites were melt mixed with PA66 using XSS-300 torque rheometer at given conditions.

Dispersity of f-MWCNTs in PA66 matrix

In order to study the distribution and the electrical conductive network of f-MWCNTs in PA66 matrix, pristine MWCNTs were also melt mixing with PA66 using the same procedure as comparison. It is clear that PA66/pristine MWCNT system has poor MWCNT dispersion and the aggregates can be seen with naked eye and TEM and SEM images (see Fig. 2 a, b), while PA66/f-MWCNT systems have better dispersions that f-MWCNTs are homogeneously dispersed, and the interfacial boundary between f-MWCNTs and PA66 matrix is practically indiscernible (see Fig. 2 c, d). As expected, the fabrication of PANI interface not only improves the dispersion of MWCNTs in PA66, but also increases the binding force between MWCNTs and PA66.

Table 1 Electrical conductivities of f-MWCNT composites versus MWCNT content

MWCNTs (%)	0	3	10	20	30	50	55	65	70	100
Conductivity (S/cm)	0.006	0.03	0.20	0.55	3.05	6.93	10.31	12.62	14.29	7.41

The electrical conductivity of PA66/f-MWCNT composites

Variation of f-MWCNT content

Figure 3 shows data of electrical conductivity versus filler content for PA66/f-MWCNTs, which exhibits a sharp transition from an insulator to a semiconductor. PA66/0.5 wt% f-MWNTs show insulator characteristic with an electrical conductivity of 10^{-14} S/cm, at the same order of magnitude with pure PA66. When the f-MWCNT content reaches 1 wt%, the electrical conductivity of PA66 composites rises rapidly to 10^{-10} S/cm, 4 orders of magnitude higher than the pure PA66. Still adding f-MWCNTs, the electrical conductivity goes up slowly and reaches a value of 10^{-5} S/cm at 10 wt% f-MWCNT amount.

In respect to CNTs/polymer composites, a well-formed conducting network is critical in deciding their conductivities. In order to explore the formation of the conducting network for PA66/f-MWCNTs, TEM images of the microtomed composites were observed at different f-MWCNT contents and shown in Fig. 4. The micrographs indicate that f-MWCNTs are well-dispersed in the polymer matrix for each concentration, as no significant agglomeration of the inclusions is observed. It is obvious that MWCNTs could not connect each other and the conducting network has not formed at a low 0.5 wt% f-MWCNT content. More conducting component, 1 wt% f-MWCNT, has induced one nanotube to begin to contact another, as Fig. 4b shows. Still adding f-MWCNTs, the conducting network is optimized and the electrical conductivity of the composite increases correspondingly. When 10 wt% f-MWCNTs are introduced to the composite, three-dimensional continuous connected network structures are generated through nanotube–nanotube and nanotube–matrix interactions resulting in an electrical conductivity of 10^{-5} S/cm, which is 8 orders of magnitude higher than the pure PA66.

Variation of mixing temperature

It is well-known that the melt mixing conditions play an important role in determining the distribution of MWCNTs in MWCNTs/polymer composites [19]. Therefore, the synthesized parameters were studied to optimize the properties of PA66/f-MWCNT composites. First, the influence of mixing temperature was investigated at fixed mixing conditions for PA66/5 wt% f-MWCNTs. The mixing temperature was varied in the range between 270 and 300 °C at a rotation speed of 100 rpm and a total mixing time of 35 min. The electrical conductivity shows a significant dependence on the mixing temperature. It increases up to more than twice with temperature increasing from 270 to 290 °C and then decreases when the temperature further increased to 300 °C (Fig. 5). Torque moments of PA66/5 wt% f-MWCNTs show a decreasing trend at higher temperature, which indicates a

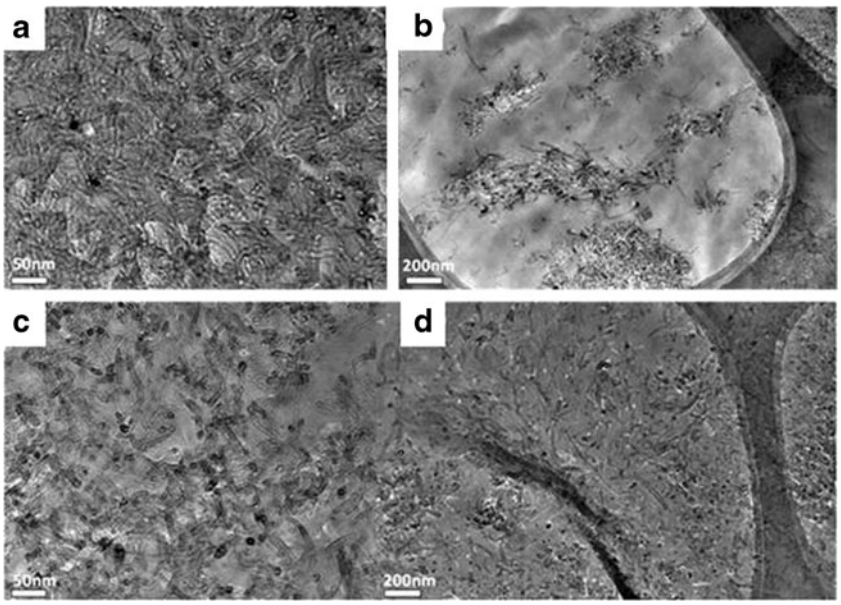

Fig. 2 TEM images of PA66 (**a**, **b**) and PA66/10 wt% f-MWCNTs (**c**, **d**) at two magnification levels. The melt mixing was conducted at 280 °C/100 rpm and the total mixing time was 35 min

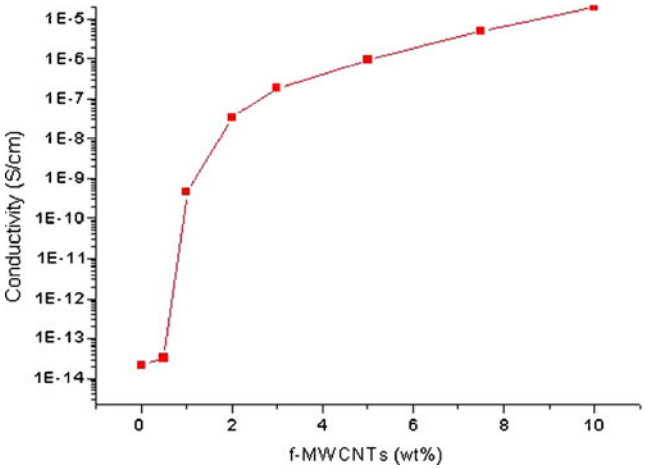

Fig. 3 Electrical conductivity of PA66/f-MWCNTs versus f-MWCNTs content

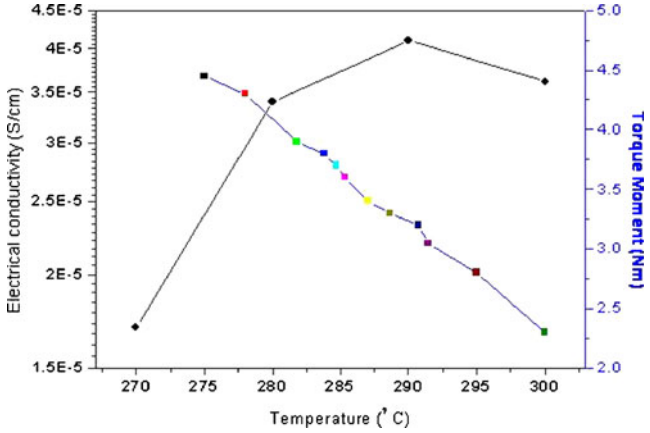

Fig. 5 Dependence of the electrical conductivity and torque moment on temperature for PA66/f-MWCNT composites

decrease in complex viscosity at higher temperature that endues better dispersion of f-MWCNTs in PA66. However, when the melting temperature reaches as high as 300 °C, the viscosity may be too low so that MWCNTs have the possibility to be disrupted, as a result, the conductivity should decrease.

Variation of mixing speed

The composites of PA66/10 wt% MWCNTs were mixed at 280 °C for 15 min, and the rotation speed was varied in the range between 25 and 100 rpm. Figure 6 shows the electrical conductivity in dependence on rotation speed. Increasing values of electrical conductivity with rising rotation speed are found. For the material melting mixed at 25 rpm, a conductivity of 10^{-6} S/cm is measured; whereas, the conductivity of composites processed at 40~150 rpm is 1 order of magnitude higher. In order to understand the changes of the electrical conductivity, the dispersion of f-MWCNTs was visualized and quantified using TEM (see Fig. 7). For the PA66 composite mixed at 25 rpm, it is obvious in Fig. 7a that the nanotubes appear to be severely agglomerated in the polymer matrix. When the mixing speed increases to 50 rpm, the dispersion of f-MWCNTs is slightly improved that many agglomerations begin to be broken. With an increased speed at 75 or 100 rpm, significant differences in the appearance of f-MWCNT dispersion (Fig. 7 c, d) could be observed that f-MWCNTs are well-dispersed in PA66 matrix and a conductive network has formed, which induces a higher conductivity of PA66/f-MWCNTs at 10^{-5} S/cm magnitude.

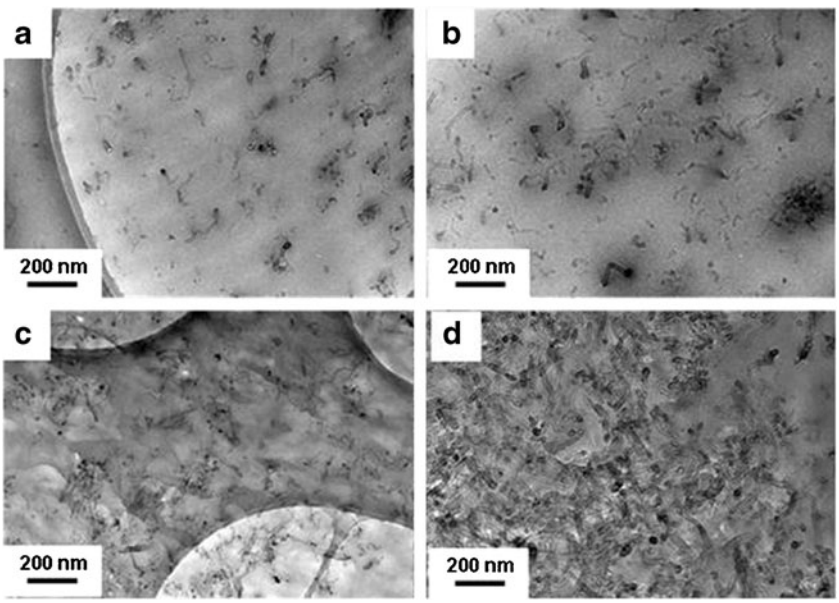

Fig. 4 TEM images of PA66/f-MWCNT composites: **a**, **b**, **c,** and **d** correspond to the f-MWCNT contents of 0.5, 1, 2, and 10 wt%, respectively

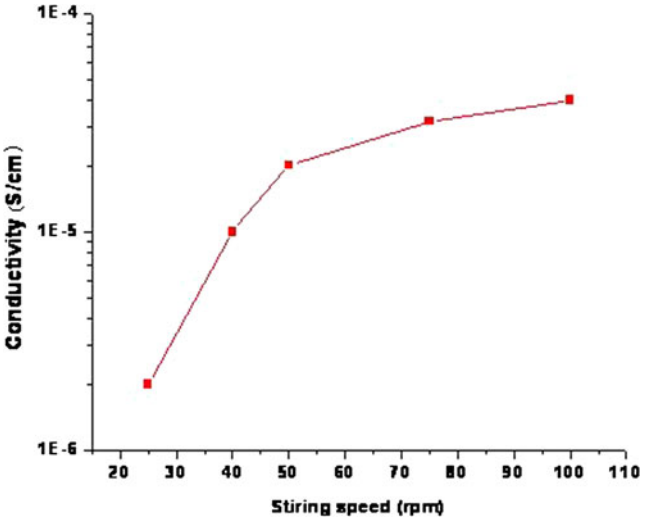

Fig. 6 Dependence of the electrical conductivity on mixing speed for PA66/f-MWCNT composites

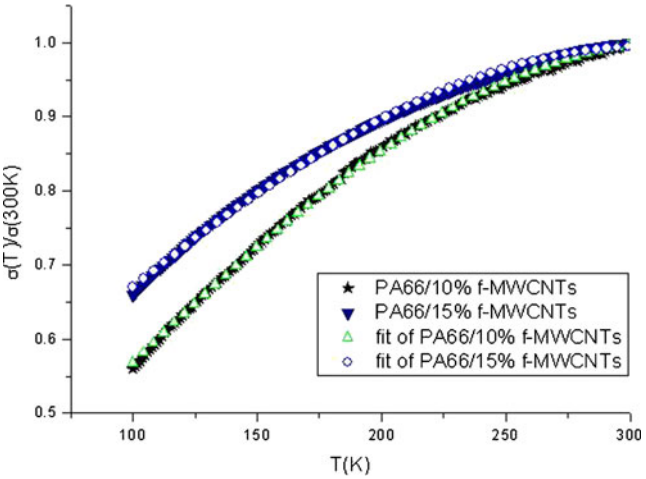

Fig. 8 Normalized temperature dependence of electrical conductivity for PA66/f-MWCNT composites. The *solid* and *dotted curves* are experimental curve and fitting curve, respectively

The electrical conducting mechanism for PA66/f-MWCNT composite

In order to explore how MWCNTs affected the composite's electrical conductivity, we studied the temperature dependence of normalized electrical conductivity, as shown in Fig. 8. The curves tell that the electrical conductivity increases as the temperature increases, indicating a semiconductor characteristic.

Best fitting can be achieved when the fluctuation-induced tunneling (FIT) model is used. According to this model, introduced by Sheng and coworkers [20, 21], electrical conductivity is ascribed to tunneling through a potential barrier of varying height due to local temperature fluctuations. The temperature dependence of $\sigma(T)$ is given by the following equation:

$$\sigma(T) = \sigma_0 \exp[-T_1/(T + T_1)] \quad (1)$$

where T_1 can be regarded as the required energy for an electron to cross the insulating gap between CNTs, T_0 is the temperature above which the thermally activated conduction over the barrier begins to occur, and σ_0 is a pre-exponential factor. The coincidence of fitting curve and experimental curve implies that Sheng's FIT model is dominant for the charge transport mechanism in PA66/f-MWCNT composites. The electrical conductivity can be attributed to the tunneling conduction through insulating PA66 barriers between MWCNT networks.

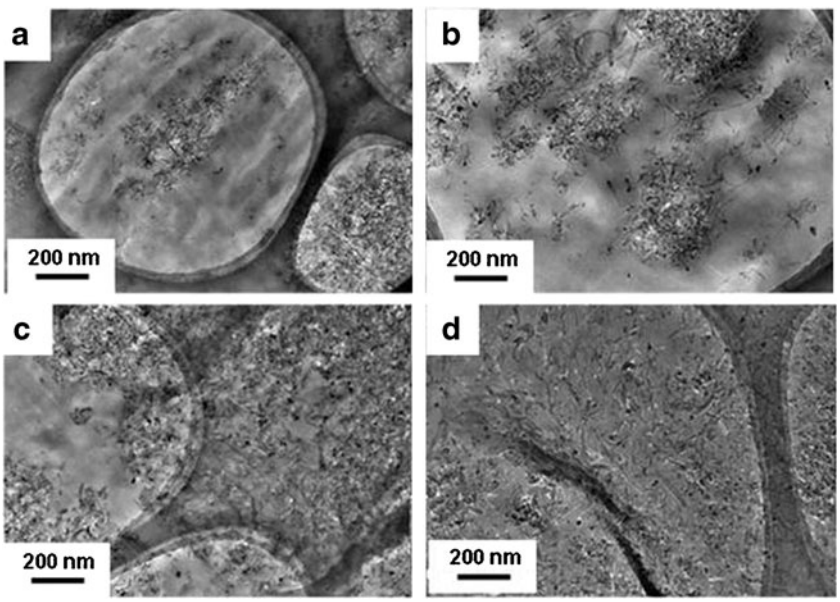

Fig. 7 TEM images of PA66/f-MWCNT composites preparing at different mixing speed: **a**, **b**, **c**, and **d** correspond to the mixing speed of 25, 50, 75, and 100 rpm, respectively

Conclusions

PANI interface was built between MWCNTs and PA66 by miniemulsion polymerization. PANI grew using MWCNTs as template, and finally, MWCNTs were covered by PANI uniformly. The strong π–π interactions between the quinoid ring of the PANI and MWCNTs were proved by FT-IR, UV, and TEM characterizations, which might facilitate charge transfer processes between the two components. The fabrication of PANI interface could not only improve the dispersion of MWCNTs, but also increase the combination between MWCNTs and PA66. Mixing conditions influenced strongly the distribution of MWCNTs and the electrical conductivity of PA66/f-MWCNTs. With increasing mixing energy input, remaining agglomerates were less in number and smaller, leading to better dispersion. A good conducting network was formed at the conditions of 10 wt% f-MWCNT content, 280 °C, and 100 rpm, which induced a high electrical conductivity of 10^{-5} S/cm, 8 orders of magnitude compared with pure PA66. Changing the experimental conditions, the electrical conductivity of PA66 composite could be tuned between 10^{-5} and 10^{-13} S/cm. Furthermore, the conducting mechanism agreed well with the FIT model that the electrical conductivity should be ascribed to tunneling through a potential barrier of varying height due to local temperature fluctuations. The present method can be extended to fabricate other conductive composites, such as polyethylene terephthalate, polymethyl methacrylate, and so on. These conductive/antistatic materials could find applications in antistatic devices, capacitors, conveyer belts for mine, and electromagnetic interference shielding fields.

Acknowledgments The authors are grateful to the support of National Natural Science Foundation of China (no. 51103160).

References

1. Zhao J, Balbuena PB (2008) J Phys Chem C 112(34):13175
2. Chakrabarti S, Gong KP, Dai L (2008) J Phys Chem C 112 (22):8136
3. Wang D, Ji WX, Li ZC, Chen L (2006) J Am Chem Soc 128:6556
4. Musumeci AW, Silva GG, Liu JW, Martens WN, Waclawik ER (2007) Polymer 48:1667
5. Sengupta R, Ganguly A, Sabharwal S, Chaki TK, Bhowmic AK (2007) J Mater Sci 42:923
6. Kim KT, Jo WH (2011) Carbon 49:819
7. Kodgire PV, Bhattacharyya AR, Bose S, Gupta N, Kulkarni AR, Misra A (2006) Chem Phys Lett 432:480
8. Haggenmueller R, Du FM, Fischer JE, Winey KI (2006) Polymer 47:2381
9. Ginic-Markovic MG, Matisons J, Cervini R, Simon GP, Fredericks PM (2006) Chem Mater 18:6258
10. Konyushenko EN, Stejskal J, Trchova M, Hradil J, Kovarova J, Prokes J (2006) Polymer 47:5715
11. Mandal S, Bhattacharyya S, Borovkov V, Patra A (2011) J Phys Chem C 115(49):24029
12. Zhang Q, Dong A, Zhai YA, Liu FQ, Gao G (2009) J Phys Chem C 113(28):12033
13. Sun Y, Wilson SR, Schuster DI (2001) J Am Chem Soc 123:5348
14. Zengin H, Zhou WS, Jin JY, Czerw R, Smith DW, Echegoyen L (2002) Adv Mater 14(20):1480
15. Quillard S, Louarn G, Lefrant S, Macdiarmid AG (1994) Phys Rev B 50:12496
16. Wu TW, Lin YW (2006) Polymer 47:3576
17. Li XH, Wu B, Huang JE, Zhang J, Liu ZF, Li HL (2002) Carbon 411:1645
18. Logakis E, Pandis C (2009) J Polym Sci part B Polym Phys 47:764
19. Sheng P (1980) Phys Rev B 21(6):2180
20. Sheng P, Sichel EK, Gittleman JL (1978) Phys Rev Lett 40 (18):1197
21. Lin YH, Chiu SP, Lin JJ (2008) Nanotechnology 19:365201